HHS Public Access

Author manuscript

Cancer Res. Author manuscript; available in PMC 2016 May 15.

Published in final edited form as:

Cancer Res. 2015 May 15; 75(10): 2049–2060. doi:10.1158/0008-5472.CAN-14-2435.

Nitrostyrene derivatives act as RXRα ligands to inhibit TNFα activation of NFκB

Zhiping Zeng[1,#], **Zhe Sun**[1,#], **Mingfeng Huang**[1,#], **Weidong Zhang**[1], **Jie Liu**[1], **Liqun Chen**[1], **Fan Chen**[1], **Yuqi Zhou**[1], **Jiacheng Lin**[1], **Fengyu Huang**[1], **Lin Xu**[1], **Zixing Zhuang**[1], **Shangjie Guo**[1], **Gulimiran Alitongbieke**[1], **Guobin Xie**[1], **Yang Xu**[1], **Bingzhen Lin**[2], **Xihua Cao**[2], **Ying Su**[1,2], **Xiao-kun Zhang**[1,2,*], and **Hu Zhou**[1,*]

[1]School of Pharmaceutical Sciences, Xiamen University, Xiamen, Fujian, China

[2]Cancer Center, Sanford-Burnham Medical Research Institute, La Jolla, California, USA

Abstract

Retinoid X receptor alpha (RXRα) and its N-terminally truncated version - tRXRα are widely implicated in cancer development and represent intriguing targets for cancer prevention and treatment. Successful manipulation of RXRα and tRXRα requires the identification of their modulators that could produce therapeutic effects. Here we report that a class of nitrostyrene derivatives bind to RXRα by a unique mechanism, of which the nitro group of nitrostyrene derivatives and Cys432 of RXRα are required for binding. The binding results in the potent activation of Gal4-DBD-RXRα-LBD transactivation. However, the binding inhibits the transactivation of RXRα homodimer, which might be due to the distinct conformation of RXRα homodimer induced by these nitrostyrene derivatives. Two RXRα point mutants with Cys432 substituted with Tyr and Trp, respectively, could mimic the bindings of two nitrostyrene derivatives and have the ability of auto-transactivation. In studying the functional consequences of the binding, we show that these nitrostyrene derivatives could potently inhibit TNFα/NFκB signaling pathway in a tRXRα dependent manner. tRXRα promotes TNFα-induced NFκB activation through its interacting with TRAF2 and enhancing TNFα-induced ubiquitination of RIP1, which is strongly inhibited by nitrostyrene derivatives. The inhibition of TNFα-induced NFκB activation results in the synergistic effect of the combination of nitrostyrene derivatives and

[*]**Corresponding Authors:** Hu Zhou, School of Pharmaceutical Sciences, Xiamen University, Xiamen, Fujian 361102, China. Phone: 86-5922182552; huzhou@xmu.edu.cn, Xiao-kun Zhang, School of Pharmaceutical Sciences, Xiamen University, Xiamen, Fujian 361102, China. Phone: 86-5922181851; xkzhang@xmu.edu.cn.
[#]These authors contributed equally to this work

Disclosure of Potential Conflicts of Interest
No potential conflicts of interest were disclosed.

Authors' Contributions
Conception and design: H. Zhou, X. Zhang
Development of methodology: H. Zhou, X. Zhang, Z. Zeng, Z, Sun, M. Huang
Acquisition of data (provided animals, acquired and managed patients, provided facilities, etc.): Z. Zeng, Z. Sun, M. Huang, W. Zhang, J. Liu, L. Chen, F. Chen, Y. Zhou, J. Lin, F. Huang, L. Xu, Z. Zhuang, S. Guo, G. Alitongbieke, G. Xie
Analysis and interpretation of data (e.g., statistical analysis, biostatistics, computational analysis): H. Zhou, Z. Zeng, Z. Sun, M. Huang
Writing, review and/or revision of the manuscript: H. Zhou, X. Zhang, Z. Zeng, Y. Su, B. Lin, X. Cao, Y. Xu
Administrative, technical or material support (i.e., reporting or organizing data, constructing databases): Z. Zeng, Z. Sun, M. Huang
Study supervision: H. Zhou, X. Zhang

TNFα on the induction of cancer cell apoptosis. Together, our results show a new class of RXRα modulators that induce apoptosis of cancer cells through their unique binding mode and new mechanism of action.

Keywords

nitrostyrene derivative; RXRα; tRXRα; TNFα; NFκB

Introduction

Retinoid X receptor alpha (RXRα) plays pleiotropic roles in the biological and pathological processes (1,2). Dysfunctions of RXRα are implicated in a number of diseases such as cancer. For examples, abnormal changes of RXRα expressions or modifications are associated with the development of prostate, skin, liver and colon cancers (3–6). Like other nuclear receptors, RXRα binds to its responsive elements to regulate gene transcription in the nucleus (7). Recently, accumulating evidence demonstrates the non-genomic actions of RXRα. For example, some apoptotic stimuli induce RXRα and Nur77 translocating from the nucleus to the cytoplasm, where they execute pro-apoptotic effects via association of Bcl-2 and transition of Bcl-2 from an anti- to a pro-apoptotic molecule (8,9). RXR was also shown to bind to the G protein Gq in a ligand-dependent manner and impair Gq-mediated Rac activation and intracellular calcium release (10).

Several small molecules have been identified as endogenous RXRα ligands such as 9-*cis*-retinoic acid (9-*cis*-RA) and docosahexaenoic acid (DHA), and many synthetic compounds also bind to RXRα selectively and exhibit RXRα-dependent effects (11). In general, RXRα ligands are constituted of three building blocks, the hydrophobic ring, a central polyene linker, and a polar motif such as carboxyl group (12). The ionic interactions and hydrogen bonds formed between the carboxyl group of 9-*cis*-RA and Arg316 residue of RXRα are essential for the binding of 9-*cis*-RA to the ligand binding pocket (LBP) of RXRα (13). Recently, some non-classical ligands have been reported to bind to RXRα in different manners. K-8008, a derivative of sulindac, binds to the surface of RXRα (14). CF31, bigelovin, and magnolol do not require Arg316 for binding to the LBP of RXRα (15–17). Thus, RXRα is subjected to modulation by diverse molecules through different mechanisms.

Tumor necrosis factor alpha (TNFα) displays a variety of physiological activities in a cell and tissue-context dependent manner. It stimulates NFκB and Akt pathways to enhance cell survival, whereas in certain contexts it provokes apoptotic events by activating caspase-8-mediated death pathway (18,19). Recently, we reported that the non-genomic action of an N-terminally truncated RXRα (tRXRα) could play a role in the crosstalk with TNFα signaling (15,20). tRXRα produced by proteolytic cleavage of full-length RXRα is highly expressed in a variety of tumor cells and tissues (21). In response to TNFα, tRXRα interacts with the p85α regulatory subunit of phosphoinositide 3-kinase (PI3K), followed by the activation of Akt to promote tumor cell growth. However, whether tRXRα could crosstalk with other TNFα-dependent signal pathways and whether small molecules could modulate its activities remain unknown.

Nitrostyrene derivatives have been identified as potent anti-cancer agents (22,23), whereas the underlying mechanisms are still elusive. In the current study, we demonstrated that nitrostyrene derivatives (Z compounds) could inhibit TNFα/NFκB signaling pathway by binding to tRXRα and blocking the interactions of tRXRα with TRAF2, leading to TNFα- and tRXRα-dependent apoptosis of cancer cells.

Materials and Methods

Reagents and antibodies

Antibodies for RXR (sc-774), PARP-1/2 (sc-7150), c-Myc (sc-40), c-Myc (sc-789), NFκB p65 (sc-8008), α-tubulin (sc-8035), ubiquitin (sc-9133) and cyclin D1 (sc-20044) were purchased from Santa Cruz Biotechnology; Antibodies for Flag (F1804) and β-actin (A2228), and 9-*cis*-RA (R4643), ATRA (R2625), Dexamethasone (D1756), T0901317 (T2320), and Rosiglitazone (R2408) were purchased from Sigma-Aldrich; Antibody for IκBα (ab32518) was from Abcam; Antibodies for cleaved Caspase-8 (#9496), p-IKKα/β (#2078), TRAF2 (#4712) and p62 (#5114) were from Cell signaling; TNFα (210-TA) was from R&D Systems; RIP1 antibody (551041) was from BD Bioscience. Propyl pyrazole triol (1426) was from Tocris Bioscience; [^{3}H]9-*cis*-RA was obtained from Amersham; Z compounds were dissolved in ddH_2O or dimethylsulfoxide respectively.

Cell culture

Cell lines were passaged for fewer than 4 months after resuscitation and were used at the fifth through tenth passage in culture for this study. MCF-7 human breast cancer and HEK293T human embryonic kidney cells were cultured in Dulbecco's Modified Eagle's Medium (Thermo Fisher Scientific) supplemented with 10% fetal bovine serum (Life Technologies) in a humidified atmosphere containing 5% CO_2 at 37°C. Cell transfections were carried out by using Lipofectamin 2000 (Invitrogen) according to the manufacture's instructions.

Mammalian one hybrid assay

HEK293T cells were cotransfected with pG5-luc reporter (Promega) together with the plasmids encoding different NR-LBDs fused with the DNA-binding domain of Gal4. One day after transfection, cells were treated with DMSO, Z compounds or ligands specific for each nuclear receptor. After 12 hours, cells were lysed by passive lysis buffer. Firefly and Renilla luciferase activities were quantitated using the Dual-Luciferase Reporter Assay System (Promega, E1960). Transfection and expression efficiency was normalized to renilla luciferase activity.

Protein expression and purification

The human RXRα-LBD (223–462) was cloned as an N-terminal histidine-tagged fusion protein in pET15b expression vector and overproduced in *Escherichia coli* BL21 DE3 strain. Briefly, cells were harvested and sonicated, and the extract was incubated with the His60 Ni Superflow resin. The protein-resin complexes were washed and eluted with imidazole. The eluent was collected and concentrated to 5 mg/mL for subsequent trials.

Ligand competition assay

RXRα-LBD protein was incubated with different concentrations of unlabeled 9-*cis*-RA, Z compounds or their derivatives in 200 ml of binding buffer (0.15 M KCl, 10 mM Tris-HCl [pH 7.4], 8% glycerol, and 0.5% CHAPS detergent) at 4°C for 1 h. [^{3}H]9-*cis*-RA was added to the tubes to a final concentration of 7.5 nM and a final volume of 300 ml and incubated overnight at 4°C. The RXRα-LBD was captured by nickel-coated beads. Bound [^{3}H]9-*cis*-RA was quantitated by liquid scintillation counting (20).

Surface plasmon resonance (SPR)

The binding kinetics between RXRα-LBD and compounds was analyzed at 25°C on a BIAcore T200 machine with CM5 chips (GE Healthcare). RXRα-LBD (20 μg/ml in 10 mM sodium acetate, pH 5) was immobilized on the CM5 chip using amine coupling procedures according to the manufacturer's instructions. A serial concentration of Z compounds ranging from 1 to 10 μM were used for the experiment at a flow rate of 20 μl/min. When the data collection was finished in each cycle, the sensor surface was regenerated with Glycine-HCl (10 mM, pH 2.5). Sensorgrams were fit globally with BIAcore T200 analysis using 1:1 Langmuir binding mode.

Isothermal titration calorimetry (ITC)

The thermodynamic properties of compounds binding to RXRα-LBD were determined using a VP-ITC titration calorimeter (MicroCal) in phosphate buffer at 25°C. The sample cell was filled with His-RXRα-LBD (50 μM in 25mM Tris-HCl, pH 7.5, 150 mM NaCl, 0.1% DMSO). The compounds were diluted to a concentration of 1 mM in the same buffer. The injection volumes were 2 μl each with injection time 4 s and a 120 s delay between each injection. The heat of dilution was obtained by injecting compounds into the same buffer and subtracted from the reaction before the fitting process.

Immunostaining, immunoblotting, co-immunoprecipitation assays and GST pull-down

Immunostaining, immunoblotting, co-immunoprecipitation and GST-pull-down assays were performed as described (8,9).

Size-exclusion chromatography assay

Size-exclusion chromatography assays were performed on an ÄktaPurifier system equipped with a HiLoad 16/600 Superdex 200-pg column (GE Healthcare). The column was pre-equilibrated with buffer [50 mM Sodium Phosphate (pH7.2), 150 mM NaCl) and RXRα-LBD protein was run at a flow rate of 1 mL/min.

MCF-7 xenografts

Nude mice (BALB/c, 4–5 weeks old) were injected subcutaneously with 100 μl MCF-7 cells (2×10^6). For drug treatment, mice were administered with Z-12 (30 mg/kg) diluted in Tween80 intragastrically once a day and TNFα (120×10^4 U/kg) diluted in phosphate-buffered saline plus 3 mg/ml bovine serum albumin intratumorally every 2 days alone or in combination after 6 days of transplantation. Body weight and tumor sizes were measured every 2 days. Mice were killed after drug treatment and tumors were removed for various

assessments. All manipulations involving live mice were approved by the Animal Care and Use Committee of Xiamen University.

Statistical analysis

Data were expressed as mean ± standard deviation (SD). Each assay was repeated in triplicate in three independent experiments. The statistical significance of the differences among the means of several groups was determined using Student's *t-test*

Results

Z compounds selectively regulate RXRα transactivation

We performed mammalian one-hybrid assay to screen for RXRα modulators using our in-house chemical library, and unexpectedly found that a nitrostyrene derivative (Z-1) selectively activated the transcriptional activity of the fusion protein Gal4-DBD-RXRα-LBD but not Gal4-DBD-RARα-LBD or Gal4-DBD-ERα-LBD (Fig. 1A and B). We then designed and synthesized a series of Z-1 derivatives designated as Z-2 to Z-12 (Supplementary Table S1). Two optimized derivatives, Z-10 and Z-12, dose-dependently activated RXRα transactivation, of which Z-10 and Z-12 at a concentration of 10 μM reached to similar and about 50% activity of 0.1 μM 9-*cis*-RA, respectively (Fig. 1A and C and Supplementary Fig. S1A). Interestingly, Z-11, which is different from Z-10 only in the position of nitrovinyl group on naphthalene, was unable to activate RXRα (Fig. 1A and C), demonstrating a strict requirement of Z compound' structure for activating RXRα. In contrast to the benzene group of Z-1, naphthalene group of Z-10 and anthracene group of Z-12 are larger aromatic groups, suggesting that larger groups induced a more favorable RXRα conformation for transactivation. The effect of Z-10 and Z-12 on RXRα transactivation was highly selective, as neither of them significantly activated the chimeric reporters of other nuclear receptors including RARα, RARγ, ERα, GR, LXRα and PPARγ (Fig. 1D and Supplementary Fig. S1B).

Nitro group is crucial for Z-10 and Z-12 binding and regulating RXRα transactivation

The regulation of RXRα transactivation by Z-10 and Z-12 prompted us to study their binding to RXRα protein *in vitro* by ligand competition assay. Similar to unlabeled 9-*cis*-RA, Z-10 and Z-12 dose-dependently competed with [^{3}H]-labeled 9-*cis*-RA for binding to RXRα-LBD, with IC_{50} at 0.28 and 0.81 μM, respectively. Interestingly, although Z-11 did not activate RXRα, it exhibited similar competition ability as Z-10 and Z-12 with an IC_{50} at 0.33 μM, implying that Z-11 bound to RXRα but induced a distinct conformation of RXRα (Fig. 2A). Our surface plasmon resonance (SPR)-based assay indicated that Z-10 and Z-12 does-dependently bound to RXRα-LBD with K_d values of 5.74 and 1.95 μM, respectively (Fig. 2B). The K_d value of Z-10 binding to RXRα-LBD measured by isothermal titration calorimetry (ITC)-based assay was 2.98 μM, which was in the same order of magnitude as that measured by SPR assay (Fig. 2C). Moreover, our assays based on differential scanning calorimetry (DSC) demonstrated that the T_m values of RXRα-LBD protein were shifted higher by Z-10, Z-11 and Z-12 (Supplementary Fig. S2A). Together, these data indicate that Z-10, Z-11 and Z-12 could bind to RXRα directly.

Different from classical RXRα ligands, Z serial compounds do not possess a carboxyl group but instead a nitro group. To examine the role of the nitro group, it was replaced with a carboxyl group (Supplementary Table S2). Ligand competition assay demonstrated that all the carboxyl derivatives (Z-10-1, Z-11-1 and Z-12-1) failed to displace [^{3}H]9-*cis*-RA from binding to RXRα-LBD (Fig. 2A). Similar results were determined by our DSC and ITC assays (Supplementary Fig. S2A and B). Consistently, the carboxyl derivatives were incapable of activating Gal4-DBD-RXRα-LBD transcriptional activity (Fig. 2D). We also replaced the nitro group of Z-10 with other functional groups including formyl, hydroxylamine, amine and cyano (Supplementary Table S3), and none of the derivatives (Z-10-2, -3, -4 and -5) could bind to or activate RXRα (Fig. 2E and Supplementary Fig. S2B and C). Taken together, these results demonstrate that the nitro group is essential for Z compounds binding to RXRα and regulating RXRα transactivation.

Z compounds bind to RXRα in a unique manner and induce distinct RXRα conformations

To investigate the effects of Z compounds on RXRα homodimer transactivation, we performed reporter assay using RXRE-luciferase reporter known to bind with RXRα homodimers (24). To our surprise, both Z-10 and Z-12 failed to induce the transactivation of RXRα homodimer. Moreover, they inhibited 9-*cis*-RA-induced transactivation (Fig. 3A). We then examined the effects of Z compounds on RXRα homodimer formation. The purified RXRα-LBD protein exhibited two bands on the native gel, of which the upper and lower bands represented homotetramers and homodimers, respectively. Similar to 9-*cis*-RA, the incubation of RXRα-LBD protein with Z-10 and Z-12 induced homodimer formation, accompanying with the reduction of tetramers. However, the homodimers induced by Z-10 and Z-12 migrated slightly slower than the control and 9-*cis*-RA-induced dimers (Fig. 3B and Supplementary Fig. S3A). Thus, Z-10 and Z-12 could induce distinct conformations of RXRα homodimers, which was also demonstrated by our assay of size-exclusion chromatography (Fig. 3C). This provided a possible explanation for the inability of Z-10 and Z-12 to activate RXRα homodimer despite their ability to induce homodimer formation. Unlike Z-10 and Z-12, Z-11 induced higher levels of RXRα-LBD oligomerization (Fig. 3B and Supplementary Fig. S3A), consisting with its inability of activating RXRα transactivation even binding to RXRα. As expected, the carboxyl derivatives did not show any effect on the formation of RXRα-LBD tetramer and dimer (Fig. 3B and Supplementary Fig. S3A). The distinct conformations induced by Z-10 and Z-12 were also illustrated by the different patterns of the cleaved RXRα-LBD fragments produced by limited proteolysis in the presence of Z-10, Z-12, DMSO, and 9-*cis*-RA (Supplementary Fig. S3B).

It was imagined that the distinct RXRα conformations induced by Z compounds resulted from their unique binding mode. Co-crystallography and mutagenesis assays have revealed that Arg316 in the LBP of RXRα is essential for 9-*cis*-RA binding (13,15). We therefore examined the role of Arg316 for Z-10 and Z-12 activity by reporter assay using Gal4-DBD-RXRα-LBD/R316E, a mutant with Arg316 substituted with Glu. While 9-*cis*-RA failed to activate the mutant, Z-10 and Z-12 strongly activated its transactivation (Fig. 3D). Consistently, Z-10 bound to RXRα-LBD/R316E protein with a K_d value of 8.30 μM (Supplementary Fig. S3D). Thus, the nitro group of Z compounds might not form ionic interactions and hydrogen bonds with Arg316, suggesting a different binding manner of Z

compounds, which was further characterized using other point mutants of Gal4-DBD-RXRα-LBD (Fig. 3E and Supplementary Fig. S3C). Neither 9-*cis*-RA nor Z compounds activated the mutants with Cys432 substituted with Gln, Trp or Tyr. However, mutation of Cys to Ser completely incapacitated Z-10 and Z-12 but not 9-*cis*-RA (Fig. 3E). Thus, Cys432 was more essential for Z compounds than for 9-*cis*-RA, and the point mutation of C432S could be used to distinguish 9-*cis*-RA from Z compounds. Consistently, Z-10 failed to bind to RXRα-LBD/C432S, C432Q and C432W (Supplementary Fig. S3D), demonstrating the crucial role of Cys432 for Z compounds binding. Sequence alignment of several nuclear receptors indicated that Cys432 was a unique residue in RXRα (Supplementary Fig. S3E), which might explain the RXRα selectivity of Z compounds. Intriguingly, substitution of Cys432 with Trp or Tyr resulted in two mutants with autoactivating ability (Fig. 3E). Structural comparison indicated that the phenol group of Tyr and the indole group of Trp are similar to the benzyl group of Z-1 and the naphthalene group of Z-10, respectively, in both the molecular size and the spacial structure (Fig. 3F). Therefore, it was imagined that the two mutations could mimic the bindings of Z-1 and Z-10, which was demonstrated by our size-exclusion chromatography assay showing that the mutant RXRα-LBD/C432W could form dimer spontaneously and our native gel electrophoresis assay showing that the similar migration rate of the mutant dimer and the Z-10-induced dimer (Fig. 3G and H).

Z-10 and Z-12 inhibit TNFα activation of the NFκB signaling pathway

We reported previously that K-80003, a Sulindac derivative, could inhibit TNFα-induced Akt activation by preventing the interaction of tRXRα and p85α (20). Unlike K-80003, Z-10 and Z-12 could not inhibit TNFα-induced interaction of tRXRα with p85α (Supplementary Fig. S4A). Instead, Z-10 dose-dependently inhibited NFκB activation by TNFα in our reporter gene assay (Supplementary Fig. S4B). Consistently, TNFα-induced expression of NFκB target genes including *c-myc*, *cyclin D1* and *p62* was inhibited by Z-10 and Z-12 (Fig. 4A). Further analysis revealed that Z-10 and Z-12 significantly inhibited TNFα-induced p65 nuclear translocation, IκBα degradation and IKKα/β phosphorylation (Fig. 4B, 4C and Supplementary Fig. S4C). We next examined whether the inhibition of NFκB activation was RXRα dependent. Compared to control siRNA, transfection of RXRα siRNA decreased the expression of both RXRα and tRXRα, which was accompanied with the impaired effect of Z compounds on TNFα-induced IκBα degradation (Supplementary Fig. S4D). The RXRα-dependent effect of Z compounds was also illustrated by our results showing that the inhibitory effect of Z-10 on TNFα-induced IκBα degradation was stronger in MCF-7 cells expressing higher levels of RXRα and tRXRα than in H460 cells with much lower RXRα and tRXRα expression (Fig. 4D). We also examined whether the effect of Z compounds could be modulated by known RXRα ligands such as 9-*cis*-RA, CD3254 and UVI3003, which did not show apparent effects on TNFα-induced IκBα degradation (Supplementary Fig. S4E). When Z compounds were used together with these known RXRα ligands, the inhibitory effects of both Z-10 and Z-12 on TNFα-induced IκBα degradation was reduced (Fig. 4E). In addition, the carboxyl derivatives, Z-10-1 and Z-12-1 incapable of binding to RXRα, did not show any effect on TNFα-induced IκBα degradation (Supplementary Fig. S4F). Taken together, these data demonstrate that Z-10 and Z-12 inhibit TNFα activation of the NFκB signaling pathway in an RXRα/tRXRα dependent manner.

Z compounds inhibit tRXRα-mediated RIP1 ubiquitination and the interaction of TRAF2 and tRXRα

To determine the molecular mechanism by which Z compounds inhibited TNFα activation of NFκB, we first analyzed the role of RXRα and tRXRα in this signaling pathway. Overexpression of Myc-RXRα/Δ80 (representing tRXRα) but not Myc-RXRα in MCF-7 cells significantly enhanced both the basal and TNFα-stimulated NFκB transcriptional activity and IκBα degradation (Supplementary Fig. S5A and B). TRAF, the IKK upstream transducer of TNFα/NFκB signal pathway, is an essential component in this pathway (25). Ectopic expression of TRAF2 slightly activated NFκB transcription and IκBα degradation, which was dramatically enhanced by transfection of Myc-RXRα/Δ80 but not Myc-RXRα in a dose-dependent manner (Fig. 5A and B). Thus, tRXRα but not RXRα is a positive regulator of TNFα activation of NFκB. When TRAF2 expression was suppressed by siRNA-mediated knockdown, the effect of Z-12 on inhibiting TNFα-induced IκBa degradation was dramatically reduced, indicating the role of TRAF2 in the activity of Z compounds (Fig. 5C). We then determined the possibility that tRXRα interacted with TRAF2. When Flag-TRAF2 was cotransfected with either Myc-RXRα/Δ80 or Myc-RXRα, immunoprecipitation of Flag-TRAF2 resulted in co-precipitation of Myc-RXRα/Δ80 but not Myc-RXRα, which was strongly enhanced by TNFα (Fig. 5D). Similarly, when the complex was immunoprecipitated with anti-Myc antibody, Flag-TRAF2 was detected in the immunoprecipitated complex when coexpressed with Myc-RXRα/Δ80 but not Myc-RXRα (Supplementary Fig. S5C). We also found that TNFα could induce the interaction of Myc-RXRα/Δ80 with endogenous TRAF2 (Supplementary Fig. S5D). The direct interaction of RXRα/Δ80 and TRAF2 was revealed by our GST pull-down assay (Supplementary Fig. S5E). Further analysis indicated that the N-terminal region of TRAF2 was responsible for binding to RXRα/Δ80 (Supplementary Fig. S5F). When the effect of Z-10 and Z-12 was analyzed, we found that treatment of cells with either of the compounds strongly inhibited TNFα-induced interaction of tRXRα with TRAF2 (Fig. 5E). The activation of TRAF2 often leads to the ubiquitination of RIP1, which is required for the activation of NFκB by TNFα (26,27). We found that RXRα/Δ80 could strongly promote TNFα-induced RIP1 ubiquitination, which was largely blocked by Z-10 (Fig. 5F). Together, tRXRα may contribute to the activation of NFκB pathway by TNFα through binding to TRAF2 and promoting RIP1 ubiquitination, and Z compounds may suppress tRXRα-dependent activation of the NFκB signaling pathway through their inhibition of tRXRα/TRAF2 complex formation.

Z-10 and Z-12 induce TNFα- and tRXRα-dependent cancer cell apoptosis

We hypothesized that suppression of tRXRα activation of the NFκB survival signaling by Z compounds may provoke the apoptotic potential of TNFα. Indeed, when cells were treated with TNFα together with either Z-10 or Z-12, a significant apoptosis of cells, indicated by PARP cleavage and nuclear fragmentation, was observed, which did not happen when cells were treated with Z-10, Z-12, or TNFα alone (Fig. 6A and Supplementary Fig. S6A). TNFα is known to induce caspase-8 dependent apoptosis (18), which was also revealed by our experiment (Fig. 6A). Treatment of cells with the general caspase inhibitor Z-VAD-FMK completely blocked the PARP cleavage induced by the combination of TNFα and Z compounds (Supplementary Fig. S6B). Thus, Z compounds are able to activate the death

effect of TNFα. Consistently, TNFα combination with Z-10 exhibited much stronger inhibitory effects on MCF-7 cell colony formation than either of them alone (Fig. 6B).

In contrast to the effect of Z compounds, 9-*cis*-RA, CD3254 and UVI3003 showed little effect on inducing PARP cleavage in the presence of TNFα (Supplementary Fig. S6C). However, they were able to suppress the apoptotic effect of the combination of TNFα and Z compound (Fig. 6C), suggesting the involvement of RXRα in the apoptotic induction of the combination. This was first confirmed by RXRα siRNA experiments, showing that transfection of RXRα siRNA prevented PARP cleavage induced by the combination of TNFα and Z compounds (Supplementary Fig. S6D). In addition, the expression levels of RXRα and tRXRα in SW480, H460 and MCF-7 cells were directly correlated to the apoptotic status of the cells treated by TNFα/Z-10 combination (Fig. 6D). For comparison, Z-10-1 and Z-12-1 did not show any synergistic pro-apoptotic effects when used together with TNFα (Supplementary Fig. S6E). To further distinguish the role of RXRα and tRXRα, we stably transfected RXRα and RXRα/Δ80 in MCF-7 cells and examined the apoptosis of the resulting stable cell lines treated by the TNFα/Z compound combination. Compared to the parental MCF-7 cells, RXRα/Δ80 but not RXRα stable cell line showed increased apoptosis when treated with either TNFα/Z-10 or TNFα/Z-12 combination (Fig. 6E and Supplementary Fig. S6F). Similarly, we observed RXRα/Δ80- but not RXRα-dependent nuclear fragments induced by the TNFα/Z-10 combination (Supplementary Fig. S6G). Together, these data demonstrate that the combination of TNFα and Z compounds induces a tRXRα-dependent apoptosis of MCF-7 cancer cells.

When Flag-TRAF2 was overexpressed in MCF-7 cells, the synergistic effects of TNFα and Z-10 on inducing PARP cleavage was largely blocked (Fig. 6F). In contrast, overexpression of dominant-negative TRAF2 (dnTRAF2) stimulated TNFα-induced PARP cleavage, which was not enhanced by Z-10 (Fig. 6G). These data suggested that the inhibition of TNFα/NFκB signaling by Z compounds led to the activation of TNFα apoptotic pathway, providing an explanation for the synergistic pro-apoptosis effects of the combination. We further evaluated whether Z compounds alone or combination with TNFα inhibited MCF-7 cell growth *in vivo*. After subcutaneous injection of MCF-7 cells, we treated mice with vehicle, Z-12, TNFα or TNFα/Z-12 by irrigation of Z compounds and intratumoral injection of TNFα. In MCF-7 bearing mice, TNFα/Z-12 combination induced significant suppression of tumor growth when compared to vehicle, Z-12, and TNFα (Fig. 6H). The pronounced delay in tumor growth, especially by the treatment of TNFα/Z-12 combination, was translated into tumor weight values, which was obtained at the end of the treatment (Fig. 6I). Tumor growth inhibition and extensive apoptosis of cancer cells were also observed when mice were treated with Z-10 or Z-12 alone (Fig. 6H and I and Supplementary Fig. S6H, I and J), likely due to the self-produced TNFα of tumor tissues.

Discussion

By using a variety of *in vitro* and *in vivo* approaches, we showed that several nitrostyrene derivatives could bind to RXRα through a new mechanism (Fig. 2 and 3 and Supplementary Fig. S2 and S3). It has been reported that synthetic nitro-compounds T0070907 and GW9662 are PPARγ antagonists (28). Endogenous nitro-fatty acids including nitrated

linoleic acid (LA-NO_2) and nitrated oleic acid (OA-NO_2) are also identified as robust PPARγ agonists, which induce PPARγ-dependent effects including macrophage CD-36 expression, adipocyte differentiation, and glucose uptake (29,30). Several other nuclear receptors such as ER and HNF4α were also found to bind to nitro compounds (31,32). However, to our knowledge, Z compounds are the first identified nitro-ligands for RXRα. Since the variety of the nitrated lipid acids and other nitrated small molecules exist in the body (33), it is much likely there are endogenous nitro-ligands of RXRα, which is worthy of further investigation.

It has been reported that a replacement of nitro group with carboxyl group abolishes the effects of nitrostyrene derivatives on pro-apoptotic induction (34), antiplatelet activity and inhibiting NLRP3 inflammasome activation (35,36). Here we also demonstrated that nitro group was essential for Z compounds to bind to RXRα (Fig. 2A and Supplementary Fig. S2), stimulate RXRα transactivation (Fig. 2D and E), regulate RXRα oligomerization (Fig. 3B and Supplementary Fig. S3A), inhibit TNFα activation of NFκB (Supplementary Fig. S4F), and induce cancer cell apoptosis (Supplementary Fig. S6E). Therefore, nitro group is critical for the nitrostyrene derivatives to exert their wide biological activities, which is partly due to the requirement of nitro group for nitrostyrene derivatives binding to RXRα (Fig. 2 and Supplementary Fig. S2).

Crystallographic analysis indicates that amino acid residues responsible for interacting with LA-NO_2 and rosiglitazone are different, leading to distinct conformational changes of PPARγ-LBD when complexed with LA-NO_2 and rosiglitazone (37). Similarly, Z compounds induced distinct conformations of RXRα homodimer (Fig. 3B and C and Supplementary Fig. S3A and B). Our mutagenesis study indicated that Cys432, which is located at the corner of the L shape LBP (13,38), was essential for Z compounds to activate and bind to RXRα (Fig. 3E and Supplementary Fig. S3C and D). The distinct conformations of RXRα induced by Z compounds may rely on their unique interaction with Cys432, which was in part supported by the self-activation of RXRα mutants C432Y and C432W mimic the binding of Z compounds (Fig. 3E, F, G, and H). The importance of Cys432 for specific ligand binding and activity has been illustrated by an early report. Tributyltin, an organotin compound, is able to induce an active conformation of RXRα-LBD, primarily due to the covalent bond formed between tin atom and Cys432 (39).

Crystallographic analysis demonstrates that hydrogen bonds formed between nitro group and residues Arg288 or Glu343 stabilize the complex of LA-NO_2 and PPARγ (37), while spectrometric analysis indicates that OA-NO_2 covalent binds PPARγ by Michael addition of Cys285 with nitroalkene (40). Our SPR results showed the quick dissociation of Z compounds from RXRα-LBD in the dissociation phase (Fig. 2B), implying no strong covalent binding between Z compounds and RXRα. However, we could not exclude the possibility that Z compounds bind to RXRα through a weak covalent binding via the Michael addition of Cys432 with nitroalkene, which might be microenvironment-sensitive (in RXRα LBP) and reversible referring to the nitroalkylation reactions (41).

tRXRα is able to bind to p85α to enhance TNFα-stimulated Akt activation and cancer growth (20). In this study, we showed that tRXRα could also enhance TNFα activation of

the NFκB signaling probably through its interaction with TRAF2 and induction of RIP1 ubiquitination (Fig. 5 and Supplementary Fig. S5). Interestingly, TNFα promoted the interaction of TRAF2 with tRXRα but not RXRα (Fig. 5D and F and Supplementary Fig. S5C and D), suggesting a possible mechanism by which abnormal activation of the TNFα/NFκB pathway plays a role in mediating the tumor promoting effect of tRXRα that is specifically produced in cancer cells (15,20). Such a tRXRα-mediated activation of the NFκB pathway may provide a new direction for targeting tRXRα through inhibiting its interactions with TRAF2. Indeed, our data showed that Z compounds strongly inhibited TNFα-induced interaction of TRAF2 with tRXRα and RIP1 ubiquitination (Fig. 5E and F), which was associated with their inhibition of the TNFα/NFκB signaling pathway in a tRXRα-dependent manner (Fig. 4D and E and Supplementary Fig. S4D). Unlike Sulindac and its derivatives (20), Z compounds did not inhibit tRXRα interaction with p85α (Supplementary Fig. S4A), reflecting the different tRXRα conformations induced by nitrostyrene derivatives and Sulindac derivatives.

Suppression of the TNFα/NFκB signaling pathway may convert TNFα from a tumor promoter to a tumor suppressor (42,43). Indeed, the potent effects of Z compounds on inhibiting TNFα/NFκB survival pathway resulted in a synergistic effect of Z compounds and TNFα on inducing tumor cell apoptosis (Fig. 6 and Supplementary Fig. S6), likely due to the activation of the TNFα-mediated pathway of apoptosis (Fig. 6A and Supplementary Fig. S6B). The synergistic anti-tumor effect of the combination was tRXRα dependent (Fig. 6C, D and E and Supplementary Fig. S6D), consistent with the facts that Z compounds bound to RXRα and inhibited TNFα activation of NFκB in a tRXRα-dependent manner. Thus, our results define a class of compounds that could convert TNFα signaling from survival to death in cancer cells by targeting tRXRα-mediated TNFα/NFκB signaling pathway.

Generally, the molecular weight of RXRα ligands ranges from 300 to 500 Da determined by the effective binding and spacial size of RXRα-LBP (2,11). The sizes of Z compounds (Z-10, 199 Da; Z-12, 249 Da) are relatively small and it was imagined that Z compounds only partially occupied RXRα-LBP, which might also explain that the binding affinity of Z compounds fall into the μM but not nM range. However, the μM working concentrations of Z compounds for binding to RXRα, inducing RXRα conformational changes, inhibiting TNFα activation of NFκB, and promoting cancer cell apoptosis were in the same order of magnitude, reflecting the relevance of their binding to RXRα and their tRXRα-dependent physiological functions. The small size of Z compounds also makes it possible to optimize them. One of the optimizing approaches is to increase their molecular sizes to enhance the van der waals interactions between Z compounds and the LBP of RXRα, and the other one is to introduce a carboxyl group in appropriate positions of Z compounds to interact with Arg316, referring to the molecular basis of the interaction between LA-NO_2 and PPARγ-LBD (37).

Taken together, our results identify the first nitro-ligands of RXRα with unique RXRα binding mode and tRXRα-dependent abilities of anti-NFκB activation and pro-apoptosis of cancer cells. Our results also reveal a new mechanism by which tRXRα promotes tumor

growth, providing a new strategy for inhibiting TNFα activation of the NFκB pathway by targeting tRXRα.

Supplementary Material

Refer to Web version on PubMed Central for supplementary material.

Acknowledgments

Grant Support

This work was supported by the grants from the National Nature Science Fund of China (NSFC-31471318, NSFC-31271453, NSFC-91129302 and NSFC-81301888), the Fundamental Research Funds for the Central Universities (2013121038), Xiamen science and technology project (3502Z20123015), the National Institutes of Health (CA140980, GM089927), the U.S. Army Medical Research and Material Command (W81XWH-11-1-0677) and the California Breast Cancer Research Program (20IB-0138).

References

1. Szanto A, Narkar V, Shen Q, Uray IP, Davies PJ, Nagy L. Retinoid X receptors: X-ploring their (patho)physiological functions. Cell Death Differ. 2004; 11(Suppl 2):S126–S143. [PubMed: 15608692]
2. de Lera AR, Bourguet W, Altucci L, Gronemeyer H. Design of selective nuclear receptor modulators: RAR and RXR as a case study. Nat Rev Drug Discov. 2007; 6(10):811–820. [PubMed: 17906643]
3. Huang J, Powell WC, Khodavirdi AC, Wu J, Makita T, Cardiff RD, et al. Prostatic intraepithelial neoplasia in mice with conditional disruption of the retinoid X receptor alpha allele in the prostate epithelium. Cancer Res. 2002; 62(16):4812–4819. [PubMed: 12183441]
4. Li M, Indra AK, Warot X, Brocard J, Messaddeq N, Kato S, et al. Skin abnormalities generated by temporally controlled RXRalpha mutations in mouse epidermis. Nature. 2000; 407(6804):633–636. [PubMed: 11034212]
5. Matsushima-Nishiwaki R, Okuno M, Adachi S, Sano T, Akita K, Moriwaki H, et al. Phosphorylation of retinoid X receptor alpha at serine 260 impairs its metabolism and function in human hepatocellular carcinoma. Cancer Res. 2001; 61(20):7675–7682. [PubMed: 11606411]
6. Yamazaki K, Shimizu M, Okuno M, Matsushima-Nishiwaki R, Kanemura N, Araki H, et al. Synergistic effects of RXR alpha and PPAR gamma ligands to inhibit growth in human colon cancer cells--phosphorylated RXR alpha is a critical target for colon cancer management. Gut. 2007; 56(11):1557–1563. [PubMed: 17604322]
7. Hegele RA. Retinoid X receptor heterodimers in the metabolic syndrome. N Engl J Med. 2005; 353(19):2088. [PubMed: 16282190]
8. Lin B, Kolluri SK, Lin F, Liu W, Han YH, Cao X, et al. Conversion of Bcl-2 from protector to killer by interaction with nuclear orphan receptor Nur77/TR3. Cell. 2004; 116(4):527–540. [PubMed: 14980220]
9. Cao X, Liu W, Lin F, Li H, Kolluri SK, Lin B, et al. Retinoid X receptor regulates Nur77/TR3-dependent apoptosis [corrected] by modulating its nuclear export and mitochondrial targeting. Mol Cell Biol. 2004; 24(22):9705–9725. [PubMed: 15509776]
10. Moraes LA, Swales KE, Wray JA, Damazo A, Gibbins JM, Warner TD, et al. Nongenomic signaling of the retinoid X receptor through binding and inhibiting Gq in human platelets. Blood. 2007; 109(9):3741–3744. [PubMed: 17213293]
11. Dawson MI, Xia Z. The retinoid X receptors and their ligands. Biochim Biophys Acta. 2012; 1821(1):21–56. [PubMed: 22020178]
12. Altucci L, Leibowitz MD, Ogilvie KM, de Lera AR, Gronemeyer H. RAR and RXR modulation in cancer and metabolic disease. Nat Rev Drug Discov. 2007; 6(10):793–810. [PubMed: 17906642]

13. Egea PF, Mitschler A, Rochel N, Ruff M, Chambon P, Moras D. Crystal structure of the human RXRalpha ligand-binding domain bound to its natural ligand: 9-cis retinoic acid. EMBO J. 2000; 19(11):2592–2601. [PubMed: 10835357]
14. Chen L, Wang ZG, Aleshin AE, Chen F, Chen J, Jiang F, et al. Sulindac-Derived RXRalpha Modulators Inhibit Cancer Cell Growth by Binding to a Novel Site. Chem Biol. 2014
15. Wang GH, Jiang FQ, Duan YH, Zeng ZP, Chen F, Dai Y, et al. Targeting truncated retinoid X receptor-alpha by CF31 induces TNF-alpha-dependent apoptosis. Cancer Res. 2013; 73(1):307–318. [PubMed: 23151904]
16. Zhang H, Li L, Chen L, Hu L, Jiang H, Shen X. Structure basis of bigelovin as a selective RXR agonist with a distinct binding mode. J Mol Biol. 2011; 407(1):13–20. [PubMed: 21262235]
17. Zhang H, Xu X, Chen L, Chen J, Hu L, Jiang H, et al. Molecular determinants of magnolol targeting both RXRalpha and PPARgamma. PLoS One. 2011; 6(11):e28253. [PubMed: 22140563]
18. Karin M, Lin A. NF-kappaB at the crossroads of life and death. Nat Immunol. 2002; 3(3):221–227. [PubMed: 11875461]
19. Croft M, Benedict CA, Ware CF. Clinical targeting of the TNF and TNFR superfamilies. Nat Rev Drug Discov. 2013; 12(2):147–168. [PubMed: 23334208]
20. Zhou H, Liu W, Su Y, Wei Z, Liu J, Kolluri SK, et al. NSAID sulindac and its analog bind RXRalpha and inhibit RXRalpha-dependent AKT signaling. Cancer Cell. 2010; 17(6):560–573. [PubMed: 20541701]
21. Gao W, Liu J, Hu M, Huang M, Cai S, Zeng Z, et al. Regulation of proteolytic cleavage of retinoid X receptor-alpha by GSK-3beta. Carcinogenesis. 2013; 34(6):1208–1215. [PubMed: 23389291]
22. Fathi AR, Krautheim A, Kaap S, Eger K, Steinfelder HJ. Michael adducts of ascorbic acid as inhibitors of protein phosphatase 2A and inducers of apoptosis. Bioorg Med Chem Lett. 2000; 10(14):1605–1608. [PubMed: 10915062]
23. Park J, Pei D. trans-Beta-nitrostyrene derivatives as slow-binding inhibitors of protein tyrosine phosphatases. Biochemistry. 2004; 43(47):15014–15021. [PubMed: 15554709]
24. Zhang XK, Lehmann J, Hoffmann B, Dawson MI, Cameron J, Graupner G, et al. Homodimer formation of retinoid X receptor induced by 9-cis retinoic acid. Nature. 1992; 358(6387):587–591. [PubMed: 1323763]
25. Xie P. TRAF molecules in cell signaling and in human diseases. J Mol Signal. 2013; 8(1):7. [PubMed: 23758787]
26. Ea CK, Deng L, Xia ZP, Pineda G, Chen ZJ. Activation of IKK by TNFalpha requires site-specific ubiquitination of RIP1 and polyubiquitin binding by NEMO. Mol Cell. 2006; 22(2):245–257. [PubMed: 16603398]
27. Bertrand MJ, Milutinovic S, Dickson KM, Ho WC, Boudreault A, Durkin J, et al. cIAP1 and cIAP2 facilitate cancer cell survival by functioning as E3 ligases that promote RIP1 ubiquitination. Mol Cell. 2008; 30(6):689–700. [PubMed: 18570872]
28. Burton JD, Goldenberg DM, Blumenthal RD. Potential of peroxisome proliferator-activated receptor gamma antagonist compounds as therapeutic agents for a wide range of cancer types. PPAR Res. 2008; 2008:494161. [PubMed: 18779871]
29. Schopfer FJ, Lin Y, Baker PR, Cui T, Garcia-Barrio M, Zhang J, et al. Nitrolinoleic acid: an endogenous peroxisome proliferator-activated receptor gamma ligand. Proc Natl Acad Sci U S A. 2005; 102(7):2340–2345. [PubMed: 15701701]
30. Baker PR, Lin Y, Schopfer FJ, Woodcock SR, Groeger AL, Batthyany C, et al. Fatty acid transduction of nitric oxide signaling: multiple nitrated unsaturated fatty acid derivatives exist in human blood and urine and serve as endogenous peroxisome proliferator-activated receptor ligands. J Biol Chem. 2005; 280(51):42464–42475. [PubMed: 16227625]
31. Naoum F, Kasiotis KM, Magiatis P, Haroutounian SA. Synthesis of novel nitro-substituted triaryl pyrazole derivatives as potential estrogen receptor ligands. Molecules. 2007; 12(7):1259–1273. [PubMed: 17909483]
32. Le Guevel R, Oger F, Lecorgne A, Dudasova Z, Chevance S, Bondon A, et al. Identification of small molecule regulators of the nuclear receptor HNF4alpha based on naphthofuran scaffolds. Bioorg Med Chem. 2009; 17(19):7021–7030. [PubMed: 19729315]

33. Ferreira AM, Minarrieta L, Lamas Bervejillo M, Rubbo H. Nitro-fatty acids as novel electrophilic ligands for peroxisome proliferator-activated receptors. Free Radic Biol Med. 2012; 53(9):1654–1663. [PubMed: 22982052]

34. Kaap S, Quentin I, Tamiru D, Shaheen M, Eger K, Steinfelder HJ. Structure activity analysis of the pro-apoptotic, antitumor effect of nitrostyrene adducts and related compounds. Biochem Pharmacol. 2003; 65(4):603–610. [PubMed: 12566088]

35. Wang WY, Hsieh PW, Wu YC, Wu CC. Synthesis and pharmacological evaluation of novel beta-nitrostyrene derivatives as tyrosine kinase inhibitors with potent antiplatelet activity. Biochem Pharmacol. 2007; 74(4):601–611. [PubMed: 17601492]

36. He Y, Varadarajan S, Munoz-Planillo R, Burberry A, Nakamura Y, Nunez G. 3,4-methylenedioxy-beta-nitrostyrene inhibits NLRP3 inflammasome activation by blocking assembly of the inflammasome. J Biol Chem. 2014; 289(2):1142–1150. [PubMed: 24265316]

37. Li Y, Zhang J, Schopfer FJ, Martynowski D, Garcia-Barrio MT, Kovach A, et al. Molecular recognition of nitrated fatty acids by PPAR gamma. Nat Struct Mol Biol. 2008; 15(8):865–867. [PubMed: 18604218]

38. Egea PF, Mitschler A, Moras D. Molecular recognition of agonist ligands by RXRs. Mol Endocrinol. 2002; 16(5):987–997. [PubMed: 11981034]

39. le Maire A, Grimaldi M, Roecklin D, Dagnino S, Vivat-Hannah V, Balaguer P, et al. Activation of RXR-PPAR heterodimers by organotin environmental endocrine disruptors. EMBO Rep. 2009; 10(4):367–373. [PubMed: 19270714]

40. Schopfer FJ, Cole MP, Groeger AL, Chen CS, Khoo NK, Woodcock SR, et al. Covalent peroxisome proliferator-activated receptor gamma adduction by nitro-fatty acids: selective ligand activity and anti-diabetic signaling actions. J Biol Chem. 2010; 285(16):12321–12333. [PubMed: 20097754]

41. Geisler AC, Rudolph TK. Nitroalkylation--a redox sensitive signaling pathway. Biochim Biophys Acta. 2012; 1820(6):777–784. [PubMed: 21723375]

42. Waters JP, Pober JS, Bradley JR. Tumour necrosis factor and cancer. J Pathol. 2013; 230(3):241–248. [PubMed: 23460481]

43. Chu WM. Tumor necrosis factor. Cancer Lett. 2013; 328(2):222–225. [PubMed: 23085193]

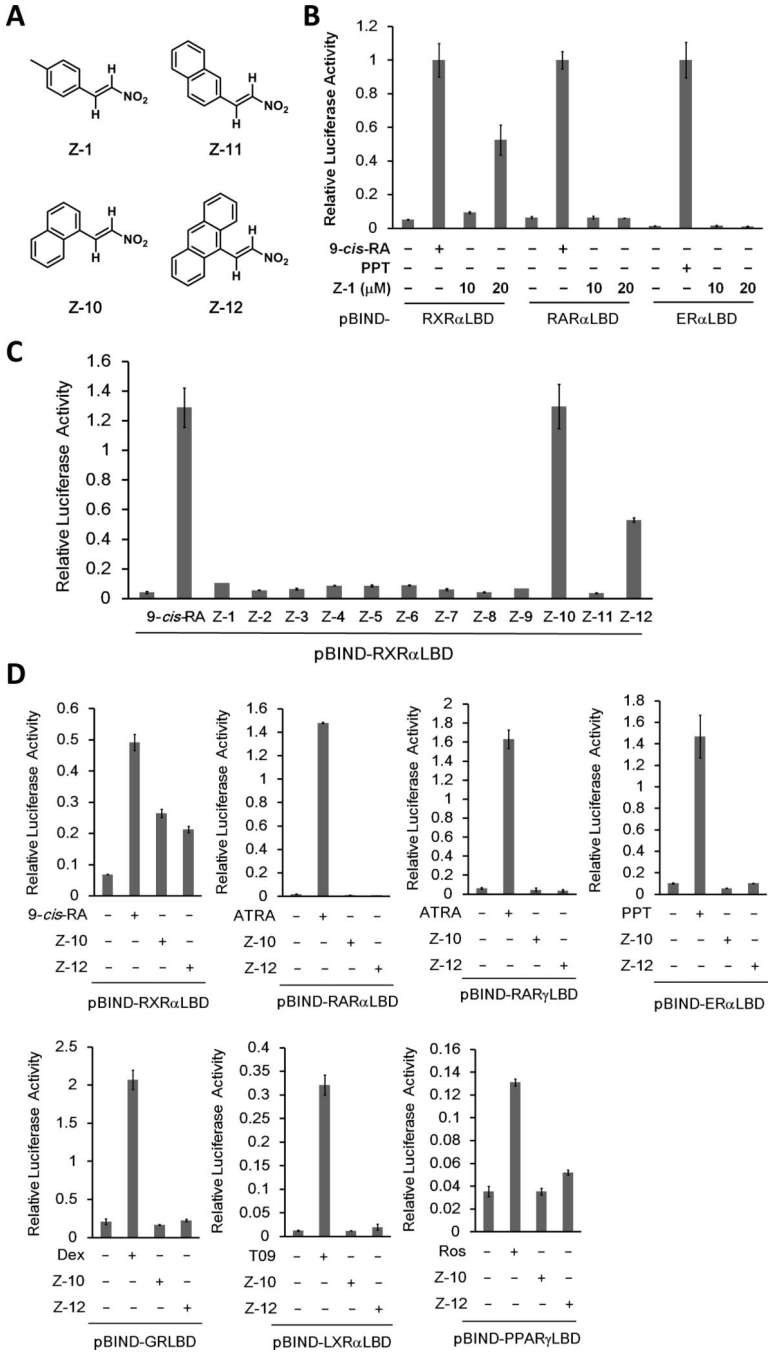

Figure 1. Z compounds selectively activate Gal4-DBD-RXRα-LBD transcriptional activity

(A) The chemical structures of Z-1 ((E)-1-methyl-4-(2-nitrovinyl)benzene), Z-10 ((E)-1-(2-nitrovinyl)naphthalene), Z-11 ((E)-2-(2-nitrovinyl)naphthalene) and Z-12 ((E)-9-(2-nitrovinyl)anthracene). **(B)** Z-1 selectively activates RXRα transcriptional activity. HEK293T cells transfected with the indicated pBIND-plasmids and pG5-luc were treated with 9-*cis*-RA (0.1 μM), PPT (10 μM) and Z-1 (10 μM) for 12 h. For all luciferase activity assays, renilla luciferase values were normalized to firefly luciferase activity and plotted as relative luciferase activity. **(C)** Z-10 and Z-12 are optimized Z-1 derivatives. HEK293T cells

transfected with pBIND-RXRα-LBD and pG5-luc were treated with 9-*cis*-RA (0.1 μM) and the indicated Z-1 derivatives (10 μM). Luciferase activities were measured 12 h post treatment and relative luciferase activity was plotted. **(D)** Z-10 and Z-12 selectively activate RXRα transcriptional activity. HEK293T cells transfected with the indicated pBIND-plasmids and pG5-luc were treated with 9-*cis*-RA (0.1 μM), ATRA (0.1 μM), PPT (10 μM), Dex (1 μM), T09 (1 μM), Ros (1 μM), Z-10 (5 μM) and Z-12 (5 μM) for 12 h, and luciferase activities were measured and normalized. Data shown are representative of at least three independent experiments. 9-*cis*-RA, 9-*cis*-retinoic acid; ATRA, all-trans retinoic acid; PPT, propyl pyrazole triol; Dex, Dexamethasone, T09, T0901317; Ros, Rosiglitazone; RXRα, retinoid X receptor α; RARα and RARγ, retinoic acid receptor α and γ, respectively; ERα, estrogen receptor α; GR, glucocorticoid receptor; LXRα, liver X receptor α; PPARγ, peroxisome proliferator-activated receptor γ.

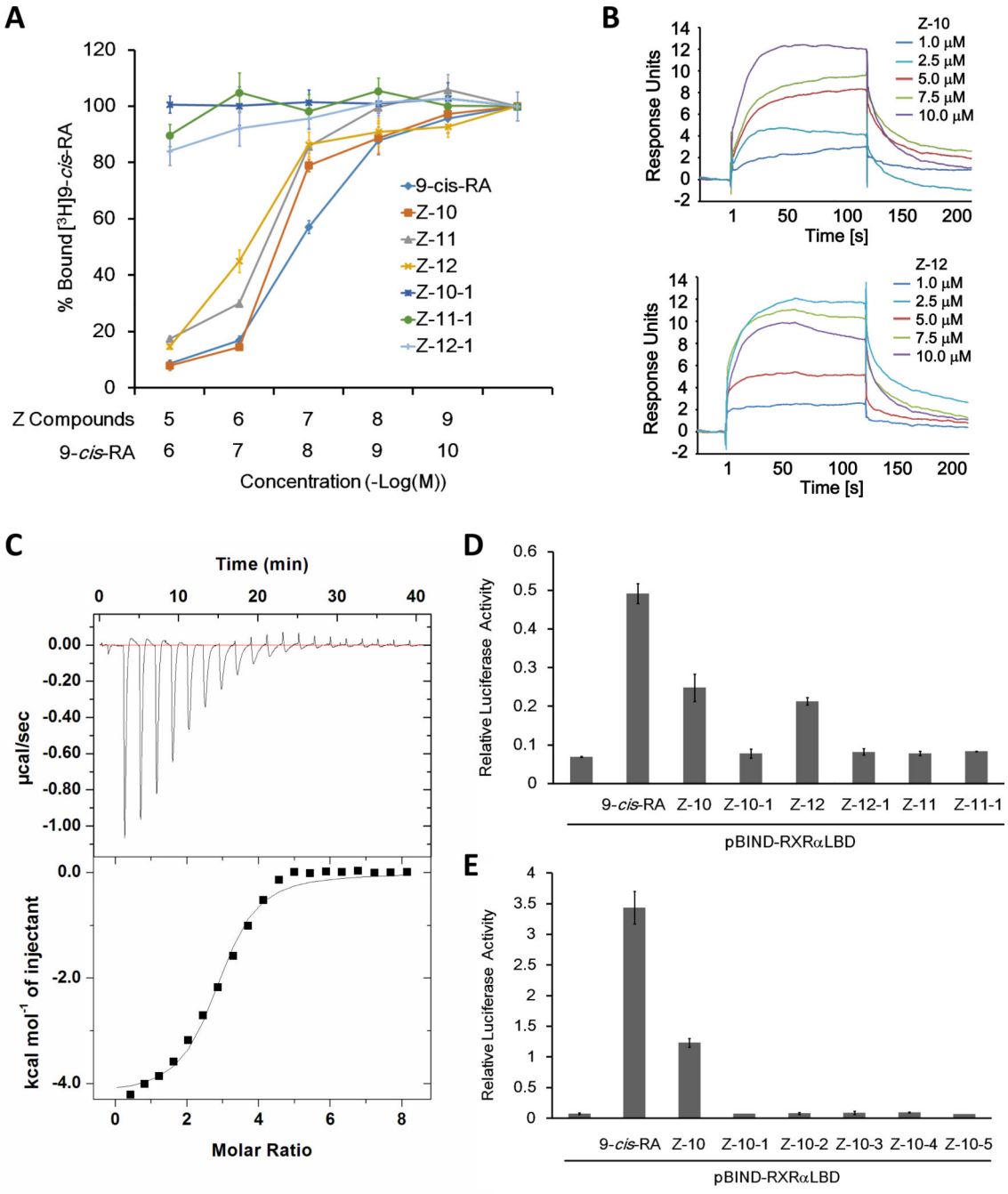

Figure 2. Nitro group is required for Z-10 and Z-12 binding to RXRα-LBD

(**A**) Z-10, Z-11 and Z-12 but not their carboxyl derivatives compete with 9-*cis*-RA binding to RXRα *in vitro*. RXRα-LBD protein was incubated with [^{3}H]9-*cis*-RA in the presence of the indicated compounds with different concentrations. Bound [^{3}H]9-*cis*-RA was quantitated by liquid scintillation counting. **(B)** The binding of Z-10 and Z-12 to RXRα-LBD is evaluated by SPR assay. The sensorgrams were obtained from injection of a series of concentration of Z-10 and Z-12 over the immobilized RXRα-LBD Chip. BIA evaluation software was used to determine the equilibrium dissociation constant (K_d). **(C)** The

thermodynamic property of Z-10 binding to RXRα-LBD is investigated by ITC assay. The upper curve in the panel showed the measured heats for each injection, while the lower plot shows the enthalpies for each injection along with the fit to a single binding site model used to estimate the K_d. All ITC data were analyzed using Origin software. **(D–E)** Nitro group is essential for Z-10 and Z-12 to induce RXRα transcriptional activity. pBIND-RXRαLBD and pG5-luc reporter were transiently transfected into HEK293T cells. Cells were treated with 9-*cis*-RA (0.1 μM), Z compounds (5 μM) and their derivatives (5 μM). Luciferase activities were measured and normalized. Data shown are representative of three independent experiments. SPR, surface plasmon resonance; ITC, isothermal titration calorimetry.

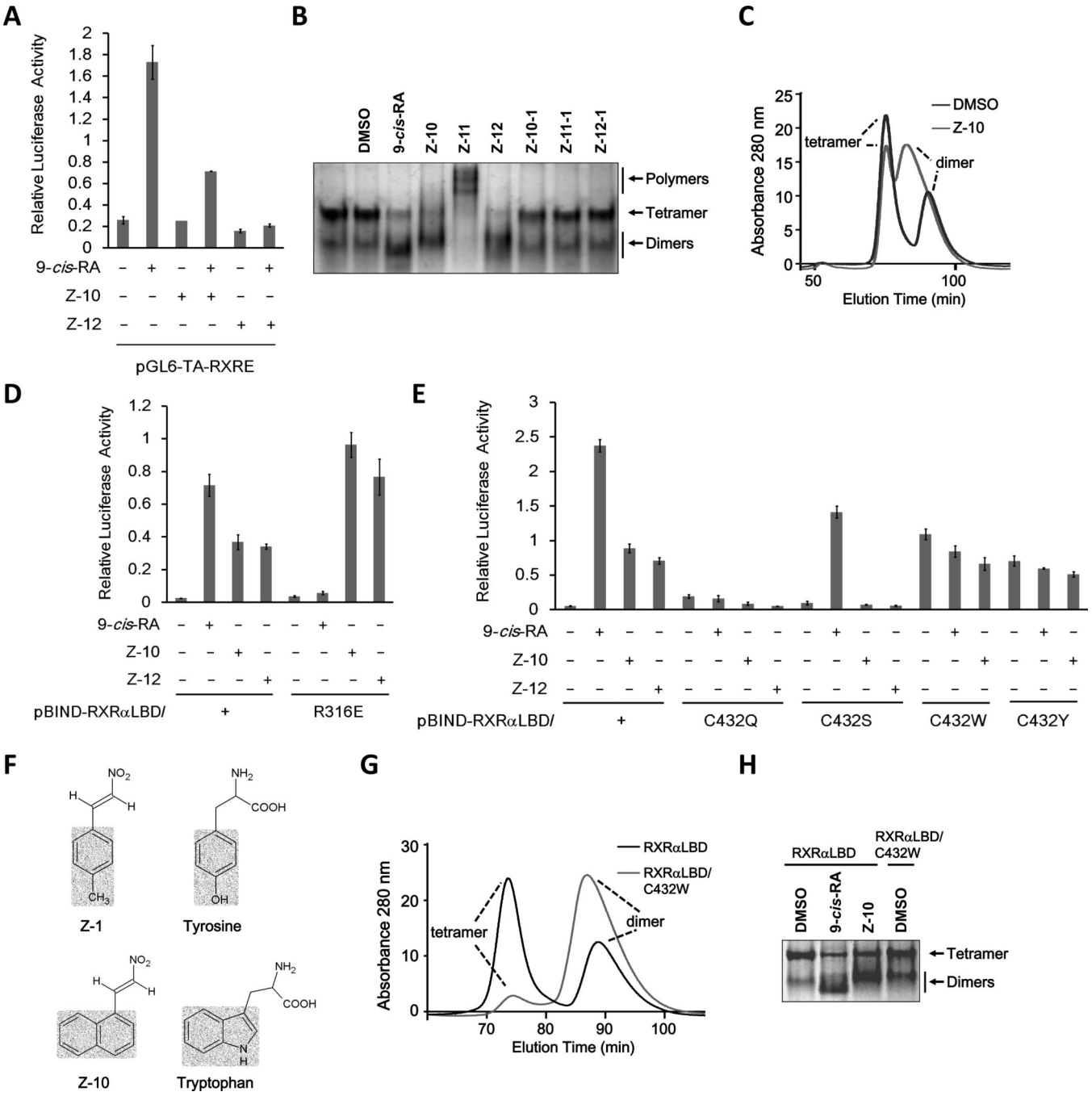

Figure 3. Z-10 and Z-12 bind RXRα in a unique manner

(A) Effect of Z-10 and Z-12 on 9-*cis*-RA-induced RXRα homodimer transactivation. HEK293T cells were cotransfected with pGL6-TA-RXRE-Luciferase and Renilla-Luciferase together with pCMV-myc-RXRα plasmid for 24 h. Cells were then treated with or without 9-*cis*-RA (0.1μM) in the presence or absence of 5 μM Z-10 and Z-12 for 12 h. Luciferase activities were measured and normalized. **(B)** Z-10 and Z-12 induce distinct conformation of RXRα-LBD homodimer. RXRα-LBD protein (0.2 μg/μl) was incubated with DMSO, 9-*cis*-RA (0.5 μM), or the indicated Z compounds (10 μM) for 3 h, and

proteins were separated by 8% non-denaturing PAGE followed by Commassie Blue staining. **(C)** Z-10 induces different homodimmers of RXRα. RXRα-LBD proteins (2 mg/ml) incubated with DMSO or Z-10 (10 μM) were analyzed by size-exclusion chromatography assay. **(D,E)** Cys432 but not R316 is required for Z-10 and Z-12 to induce RXRα transcriptional activity. HEK293T cells transfected with the indicated plasmids were treated with 9-*cis*-RA (0.1 μM), Z-10 (5 μM) or Z-12 (5 μM). Luciferase activities were measured and normalized. **(F)** Structural comparison of Z-1 and Z-10 with Tyrosine and Tryptophan. **(G)** The spontaneous formation of RXRα-LBD/C432W homodimer was analyzed by size-exclusion chromatography assay. **(H)** The homodimers of RXRα-LBD/C432W were analyzed by non-denaturing PAGE. Data shown are representative of at least three independent experiments. PAGE, polyacrylamide gel electrophoresis.

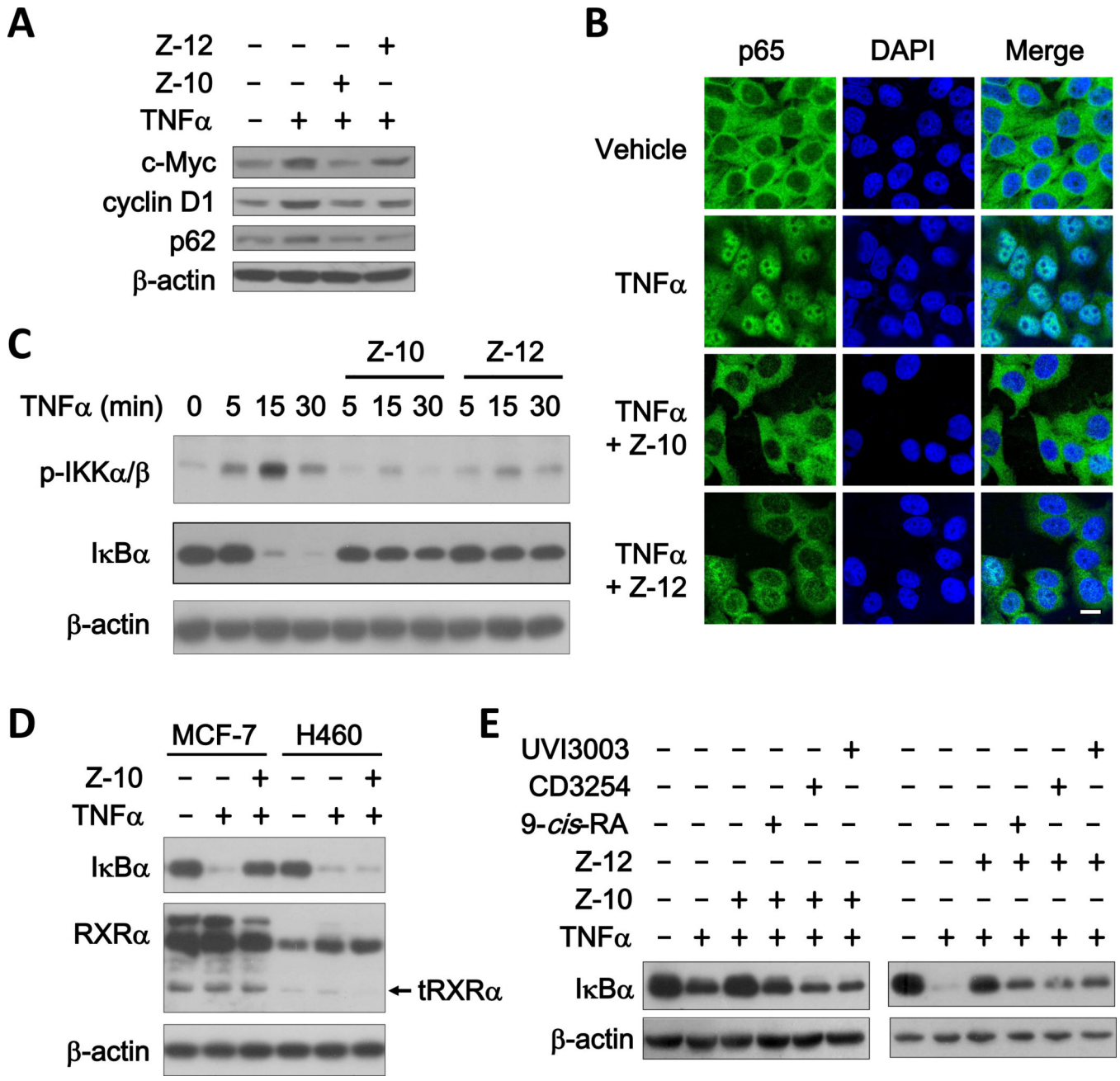

Figure 4. Z-10 and Z-12 inhibit TNFα activation of NFκB in RXRα/tRXRα dependent manner

(A) Inhibitory effect of Z-10 and Z-12 on NFκB target gene expression. MCF-7 cells were treated with TNFα (10 ng/ml) alone or together with Z-10 (10 μM) or Z-12 (10 μM) for 12 h. Protein expression levels were analyzed by immunoblotting. β-actin was used as a loading control. **(B)** Effect of Z-10 and Z-12 on TNFα-induced p65 nuclear translocation. MCF-7 cells pretreated with Z-10 (10 μM) or Z-12 (10 μM) for 1 h were exposed to TNFα (10 ng/ml) for 30 min. Cells were immunostained with anti-p65 antibody and observed by confocal microscopy (scale bar, 10 μM). **(C)** Effect of Z-10 and Z-12 on TNFα-induced IKK phosphorylation and IκBα degradation. MCF-7 cells pretreated with Z-10 (7.5 μM) or Z-12 (5 μM) for 1 h were stimulated by TNFα (10 ng/ml) for the indicated time, and IKKα/β

phosphorylation and IκBα expression were analyzed by immunoblotting. **(D)** Correlation of the inhibitory effect of Z-10 on TNFα-induced IκBα degradation and RXRα/tRXRα expression. MCF-7 or H460 cells pretreated with Z-10 (7.5 μM) for 1 h were exposed to TNFα for 30 min. The proteins were examined by immunoblotting. **(E)** RXRα ligands prevent the inhibitory effects of Z-10 and Z-12 on TNFα-induced IκBα degradation. MCF-7 cells pretreated with Z-10 (7.5 μM) and Z-12 (5 μM) alone or together with 9-*cis*-RA (0.1 μM), CD3254 (0.1 μM) and UVI3003 (1 μM) for 1 h were treated with TNFα (10 ng/ml) for 30 min. The proteins were examined by immunoblotting. Data shown are representative of at least three independent experiments. tRXRα, N-terminally truncated RXRα; TNFα, tumor necrosis factor α; IκBα, NF-Kappa-B Inhibitor α; DAPI, 4',6-diamidino-2-phenylindole.

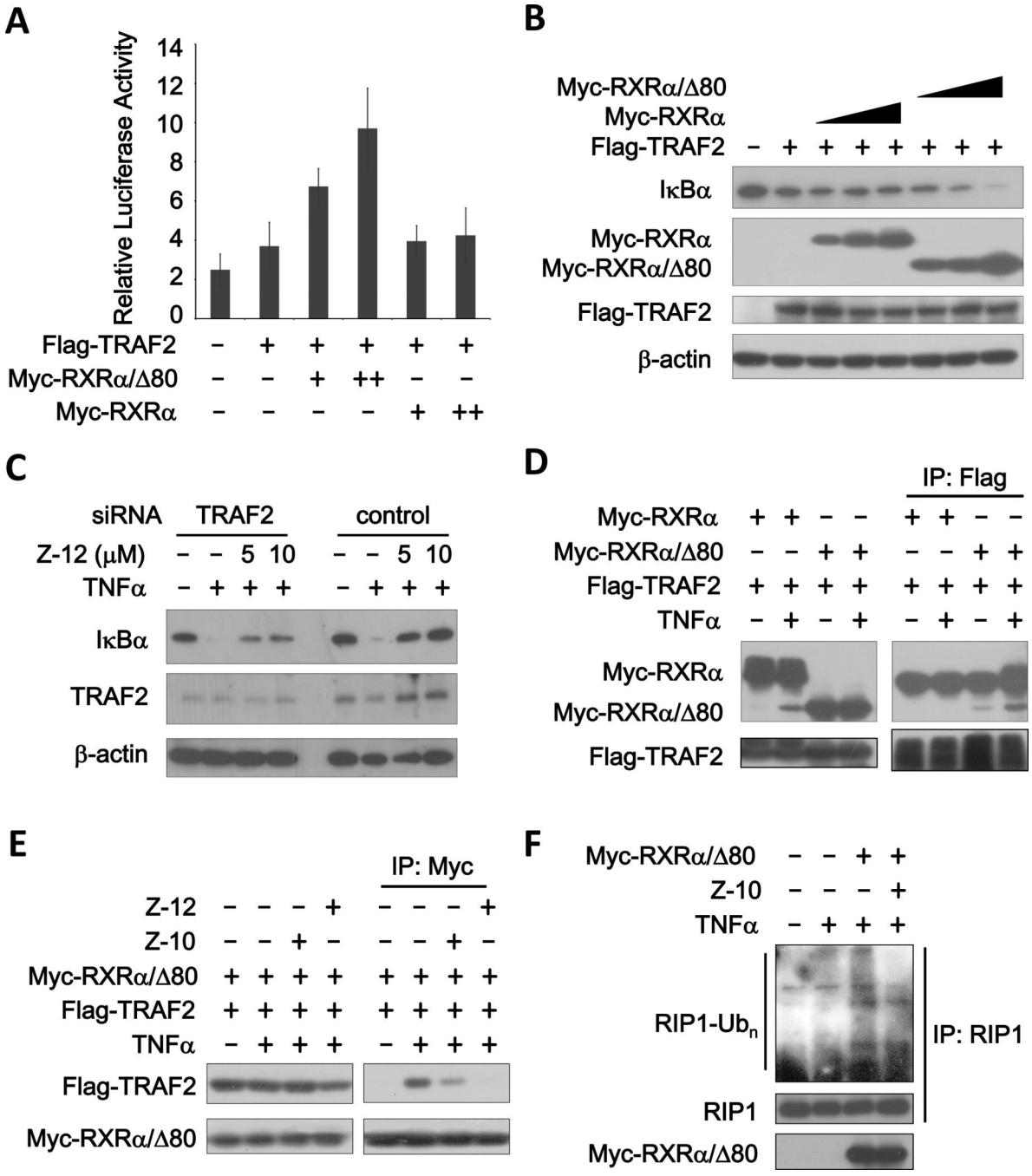

Figure 5. Z-10 and Z-12 inhibit tRXRα-mediated TNFα activation of NFκB

(A) Myc-RXRα/Δ80 but not Myc-RXRα enhances TRAF2-stimulated NFκB transactivation. MCF-7 cells were transiently transfected with NFκB-Luciferase reporter and Renilla-Luciferase with or without Myc-RXRα/Δ80 and Myc-RXRα expression plasmids for 24 h. Luciferase activities were measured and normalized. The values of Y axis are 1,000 times of relative luciferase activity. **(B)** Myc-RXRα/Δ80 but not Myc-RXRα enhances TRAF2-induced down-regulation of IκBα. MCF-7 cells were transfected with the indicated plasmids for 24 h, and cell lysates were prepared and analyzed by immunoblotting.

β-actin was used as a loading control. **(C)** Suppression of TRAF2 expression impairs the inhibitory effect of Z-12 on TNFα-induced IκBα degradation. MCF-7 cells transfected with siRNA of control or TRAF2 for 36 h were treated with Z-12 for 1 h before exposed to TNFα (10 ng/ml) for 30 min. Protein expressions were analyzed by immunoblotting. **(D)** Interaction of TRAF2 with tRXRα but not RXRα. HEK293T cells were transfected with the indicated plasmids for 24 h and then treated with TNFα (40 ng/ml) for 15 min. The complex formations were examined by co-immunoprecipitation using specific antibodies. **(E)** Effects of Z-10 and Z-12 on TNFα-induced formation of TRAF2/tRXRα complex. HEK293T cells were transfected with the indicated plasmids for 24 h and then treated with Z-10 (5 μM) and Z-12 (5 μM) for 1 h before exposed to TNFα (40 ng/ml) for 15 min. Protein interactions were analyzed by co-immunoprecipitation. **(F)** tRXRα-induced RIP1 ubiquitination is inhibited by Z-10. MCF-7 cells transfected with or without Myc-RXRα/Δ80 expression plasmids were treated with Z-10 (10 μM) for 1 h before stimulated with TNFα (20 ng/ml) for 5 min. RIP1 ubiquitination was examined by immunoprecipitated with anti-RIP1 antibody followed by immunoblotting with anti-ubiquitin antibody. Data shown are representative of at least three independent experiments. siRNA, small interference RNA; IP, immunoprecipitate.

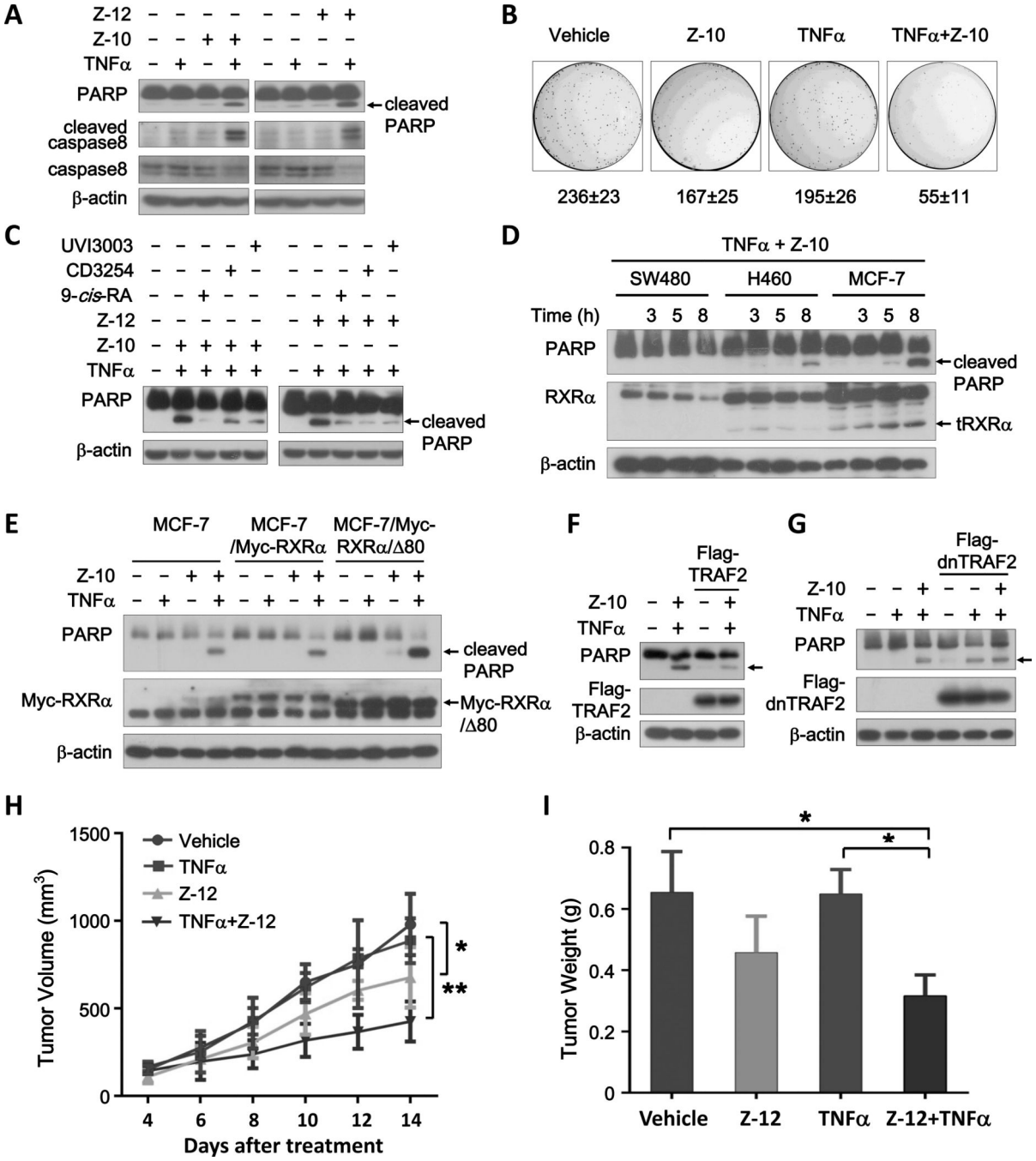

Figure 6. Z compounds and TNFα synergistically induce cancer cell apoptosis in a tRXRα-dependent manner

(**A**) Synergistic induction of PARP cleavage by TNFα combination with Z-10 or Z-12. MCF-7 cells cultured in medium with 1% fetal bovine serum were treated with Z-10 (7.5 μM), Z-12 (5 μM) and/or TNFα (10 ng/ml) for 9 h. Immunoblotting was applied to examine PARP cleavage. **(B)** Effect of Z-10 and TNFα on clonogenic survival of MCF-7 cells. **(C)** Effect of RXRα ligands on the synergistic induction of PARP cleavage by TNFα combination with Z-10 or Z-12. MCF-7 cells pretreated with 9-*cis*-RA (0.1 μM), CD3254

(0.1 μM) or UVI3003 (1 μM) for 1 h were treated with TNFα (10 ng/ml) and Z-10 (7.5 μM) or Z-12 (5 μM) for 9 h. **(D)** Correlation of the synergistic apoptotic induction of TNFα/Z-10 and RXRα/tRXRα protein levels. Cells were treated with Z-10 (7.5 μM) and TNFα (10 ng/ml) for the indicated time. **(E)** Effect of stable expression of RXRα and tRXRα on the synergistic apoptotic effect of TNFα/Z-10. Cells were treated with TNFα (10 ng/ml) and/or Z-10 (7.5 μM) for 9 h. **(F–G)** TRAF2 rescues MCF-7 apoptosis induced by Z-10 and TNFα. MCF-7 cells transfected with Flag-TRAF2 **(F)** or dominant negative TRAF2 (Flag-dn-TRAF2) **(G)** were treated with TNFα (10 ng/ml) and/or Z-10 (7.5 μM). The arrows indicate cleaved PARP. (**H–I**) Combination treatment with TNFα and Z-12 inhibits tumor growth in MCF-7 breast cancer xenograft models. Mice were treated with Z-10 (30 mg/kg) once a day by oral gavage and/or TNFα (120×10^4 U/kg) every other day after 6 days of MCF-7 cell inoculation. The tumor volume was monitored and recorded (**P*<0.05 and ***P*<0.01) **(H)**. Tumors excised at day 14 were weighed (**P*<0.05) **(I)**. Data shown are representative of at least three independent experiments. PARP, Poly (ADP-ribose) polymerase; dnTRAF2, dominant-negative TRAF2.